25th ABCM International Congress of Mechanical Engineering
October 20-25, 2019, Uberlândia, MG, Brazil

COB-2019-0150
ANALYSIS OF A PARALLEL ROBOT FOR MICRO MOVEMENTS

Mateus V. Guedes de Almeida
Fabiano Disconzi Wildner
Mário Roland Sobczyk Sobrinho
Rafael Antônio Comparsi Laranja
Universidade Federal do Rio Grande do Sul, Rua Sarmento Leite, 425, Porto Alegre—RS, Brazil, 90050-17
e-mails: mateus.vagner@gmail.com, wildner@mecanica.ufrgs.br, mario.sobczyk@ufrgs.br, rafael.laranja@ufrgs.br

Abstract. *This paper is concerned with the analysis of a parallel robot of the kind 3-revolute-prismatic-spherical (3-RPS), encompassing its inverse and direct kinematics, inverse dynamics, and workspace. The dynamics is studied using the Lagrange formulation, whereas the workspace is obtained by direct solution of the direct kinematic model. The main properties of the model are illustrated by means of simulation results.*

Keywords: *3-RPS, Parallel Robot, Kinematics, Dynamics, Workspace*

1. INTRODUCTION

Compared to their serial counterparts, parallel robots perform better in terms of precision, stiffness, and load-to-mass ratio, at the price of reduced workspace and application flexibility (Huang *et al.*, 2013). The best-known parallel mechanism is the Stewart Platform (Stewart, 1965), which is able to move on six degrees of freedom (*dof*) and is largely used in flight simulators. As presented by Clavel (1989), Gosselin and Hamel (1994), Wang and Gosselin (1997), Wang and Gosselin (1998), Li and Xu (2005), Huang *et al.* (2013), many practical applications do not require the use of all six dof, however, it is possible to develop simpler platforms to allow for significant cost reductions. Within this context, we highlight the *3-RPS* parallel mechanism, with three degrees of freedom, proposed by H. Hunt (1983). This mechanism consists of three identical linear actuators, each one with one extremity linked through a spherical joint to a movable platform, and the other to a fixed base through a rotational joint, as shown in Fig. 1(a). This work is dedicated to analyzing its main kinematic and dynamic features.

2. KINEMATICS

Kinematics of parallel robots are fundamentally different from those of serial ones (Dasgupta and Mruthyunjaya, 2000). Thus, for ease of understanding, the proposed model is presented here in a reversed order from that usually found for serial manipulators: first, the *inverse* kinematics model is discussed, whereas the *direct* one is shown afterwards.

2.1 Inverse Kinematics

The robot consists of a mobile platform $B_1B_2B_3$, a base $A_1A_2A_3$ and three extendable links, A_1B_1, A_2B_2 and A_3B_3 of lengths d_1, d_2, d_3 respectively. The three platform vertices B_1, B_2, B_3 are equally spaced by 120 degrees in a radius *h* of its center of mass *P*. Likewise, the base vertices A_1, A_2, A_3 are equally spaced the center *O*, at a distance $g \geq h$. Two coordinate systems *A(XYZ)* and *B(XYZ)* are attached to the centers of the platform and of the base, respectively, with the axis *x* is aligned with $\overline{PB_1}$, the points A_1, A_2 and A_3 are on the plane *XY* and the vector $\overline{OA_1}$ coincides with the axis *X*.

The position vectors of B_1, B_2 and B_3 with respect to the base frame *A(XYZ)* are:

$$\mathbf{q_i} = \mathbf{p} + {}^{A}_{B}\mathbf{R}\,{}^{B}\mathbf{b}_i\ , \quad i = 1, 2, 3 \tag{1}$$

where $\mathbf{p}$ is the position of the center of the moving platform, ${}^{A}_{B}\mathbf{R}$ is the rotational matrix from *A(XYZ)* to *B(XYZ)* and ${}^{B}\mathbf{b}_i$ is the position of the i^{th} vertex related to *B(XYZ)*. Applying the geometric relations shown in Fig. 1(b), Eq. (1) becomes:

$$\mathbf{q_1} = \begin{bmatrix} p_x + hu_x \\ p_y + hu_y \\ p_z + hu_z \end{bmatrix}\ , \quad \mathbf{q_2} = \begin{bmatrix} p_x - \frac{1}{2}hu_x + \frac{\sqrt{3}}{2}hv_x \\ p_y - \frac{1}{2}hu_y + \frac{\sqrt{3}}{2}hv_y \\ p_z - \frac{1}{2}hu_z + \frac{\sqrt{3}}{2}hv_z \end{bmatrix}\ , \quad \mathbf{q_3} = \begin{bmatrix} p_x - \frac{1}{2}hu_x - \frac{\sqrt{3}}{2}hv_x \\ p_y - \frac{1}{2}hu_y - \frac{\sqrt{3}}{2}hv_y \\ p_z - \frac{1}{2}hu_z - \frac{\sqrt{3}}{2}hv_z \end{bmatrix} \tag{2}$$

where $u_x, u_y, u_z, v_x, v_y, v_z$ are the director cosines of $({}^{A}_{B}\mathbf{R})$ and p_x, p_y, p_z are the elements x, y, z of $\mathbf{p}$.

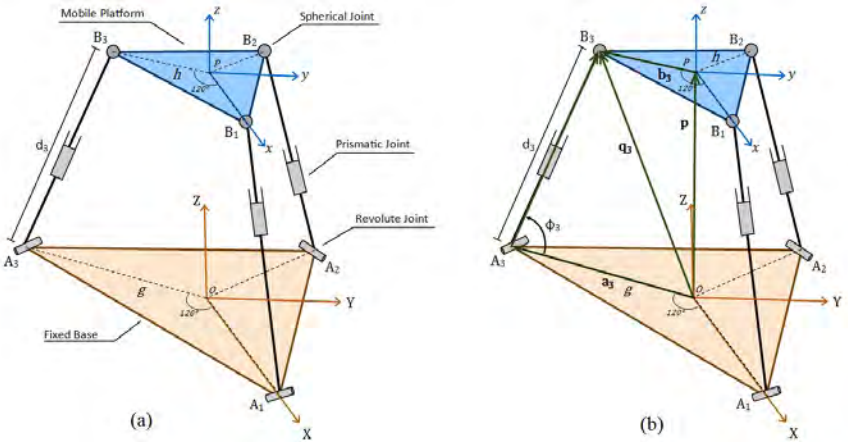

Figure 1: (a) 3-RPS mechanism. (b) Vectors of the vertices of the mechanism.

Due to the rotation joints, movement of the platform vertices on the x- and y- axes is restricted by:

$$q_{1y} = 0\ , \quad q_{2y} = -\sqrt{3}q_{2x}\ , \quad q_{3y} = \sqrt{3}q_{3x} \tag{3}$$

Therefore, from Eq. (2) and Eq. (3), one obtains the following constraint relations:

$$u_y = v_x\ , \quad p_y = -hu_y\ , \quad p_x = \frac{1}{2}h(u_x - v_y) \tag{4}$$

Alternatively, this solution can be expressed by the cosine directors in terms of Z-Y-Z Euler angles ($\gamma,\ \beta,\ \alpha$):

$$\gamma = -\alpha\ , \quad p_y = \frac{1}{2}h(1 - c\beta)c2\alpha\ , \quad p_x = -\frac{1}{2}h(1 - c\beta)s2\alpha \tag{5}$$

where $c\beta = cos(\beta)$, $c2\alpha = cos(2\alpha)$ and $s2\alpha = sin(2\alpha)$. From the restriction conditions, one concludes that three parameters must be chosen to determine the mechanism pose. However, since p_z is the only one that is completely free, it must be included in any choice set, whereas two others can be freely taken from the remaining five ($p_x,\ p_y,\ \alpha,\ \beta$ and γ). Although the mechanism has three degrees of freedom, the three Euler angles cannot be freely selected simultaneously because there are two angles that are function of each other in this case γ and α. For a given coordinate (p_x, p_y) there are two sets of Euler angles, (α, β) and (α, $-\beta$), in the order Z-Y-Z. In this paper the set (α, β) is considered. After obtaining the dependent variables, it is possible to calculate the vectors related to the legs A_iB_i with Eq.(6).

$$\mathbf{d_i} = \mathbf{q_i} - \mathbf{a_i}\ , \quad i = 1, 2, 3 \tag{6}$$

2.2 Direct Kinematics

The direct kinematics analysis is based on the relation between the lengths of the mechanism legs (d_1, d_2, d_3) and their angles with respect to the base (ϕ_1, ϕ_2, and ϕ_3), which yields:

$$\mathbf{q_1} = \begin{bmatrix} g - d_1 cos(\phi_1) \\ 0 \\ d_1 sin(\phi_1) \end{bmatrix}\ , \quad \mathbf{q_2} = \begin{bmatrix} -\frac{1}{2}(g - d_2 cos(\phi_2)) \\ \frac{\sqrt{3}}{2}(g - d_2 cos(\phi_2)) \\ d_2 sin(\phi_2) \end{bmatrix}\ , \quad \mathbf{q_3} = \begin{bmatrix} -\frac{1}{2}(g - d_3 cos(\phi_3)) \\ -\frac{\sqrt{3}}{2}(g - d_3 cos(\phi_3)) \\ d_3 sin(\phi_3) \end{bmatrix} \tag{7}$$

Due to the geometric restriction posed by the shape of the platform, the distance between two adjacent spherical joints is always $\sqrt{3}h$. Thus, applying such restriction to Eq.(7) leads to:

$$\begin{aligned} f_1 &= {d_1}^2 + {d_2}^2 + 3g^2 - 3h^2 + d_1 d_2 cos(\phi_1)cos(\phi_2) - 2d_1 d_2 sin(\phi_1)sin(\phi_2) - 3gd_1 cos(\phi_1) - 3gd_2 cos(\phi_2) \\ f_3 &= {d_2}^2 + {d_3}^2 + 3g^2 - 3h^2 + d_2 d_3 cos(\phi_2)cos(\phi_3) - 2d_2 d_3 sin(\phi_2)sin(\phi_3) - 3gd_2 cos(\phi_2) - 3gd_3 cos(\phi_3) \\ f_3 &= {d_3}^2 + {d_1}^2 + 3g^2 - 3h^2 + d_3 d_1 cos(\phi_3)cos(\phi_1) - 2d_3 d_2 sin(\phi_3)sin(\phi_1) - 3gd_3 cos(\phi_3) - 3gd_1 cos(\phi_1) \end{aligned} \tag{8}$$

The equations system described in Eq.(8) may generate up to 8 results for a given set of leg lengths d_1, d_2 and d_3, of which only one is correct for the robot ((Tsai, 1999), (Lukanin, 2005), (Ghosal, 2006)). Fig. 2 shows the 8 possible results for the equations system for a given value for d_1, d_2 and d_3 (in this case d_1 = d_2 = d_3). In practical applications this calculation is simplified by restricting the possible physical values of ϕ_1, ϕ_2, ϕ_3 which the robot can achieve due to design constraints in the prismatic joints (minimum and maximum position of the actuators) and the spherical joints (maximum possible angles).

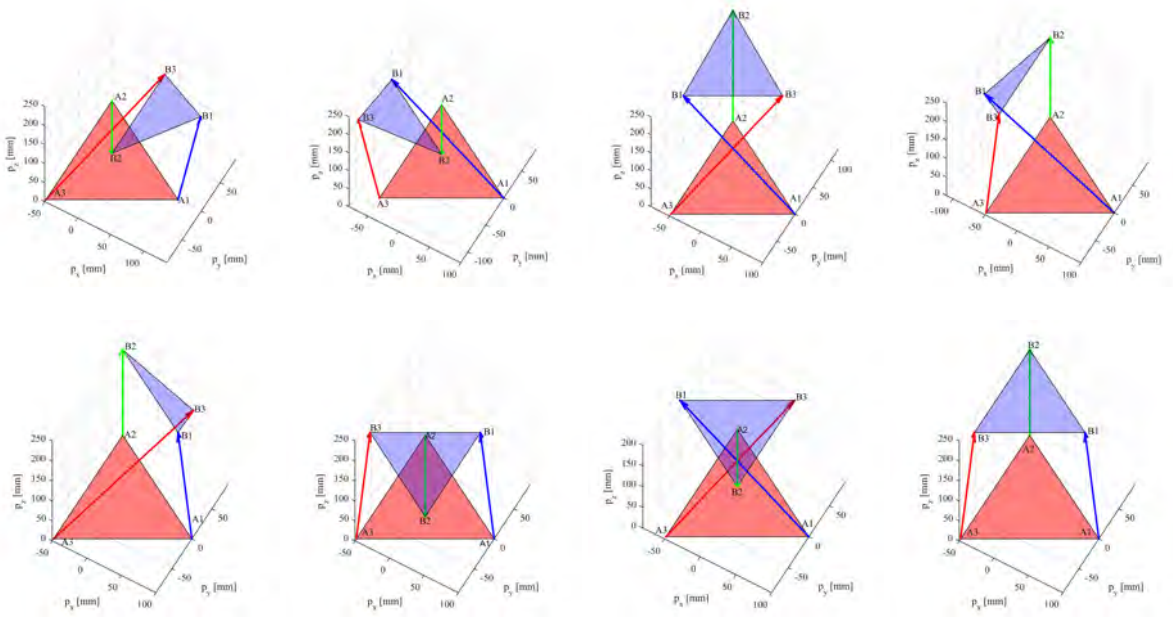

Figure 2: Eight possible results for the system equation.

3. WORKSPACE

The manipulator workspace can be obtained by calculating the inverse kinematics, but this methodology does not take into account the physical limits imposed by the joints. To include this effect, it is convenient to use the direct kinematics of the manipulator by directly specifying the values of d_1, d_2 and d_3. From the analysis performed by Sokolov (2013), it can be shown that the workspace of the centroid of the platform is limited in the plane X-Y by the cylinder with a radius equal to h (the platform radius). This limitation is independent of the maximum length provided by the prismatic joints, i.e., such cylinder has an infinite p_z coordinate, and this approach does not take into account singular positions reached by the mechanism. The Fig. 3 shows the initial position where $p_x = p_y = 0$ and the limit positions, where the centroid of the moving platform reach the surface of the theoretical cylinder for a mechanism with $h = 120\,mm$.

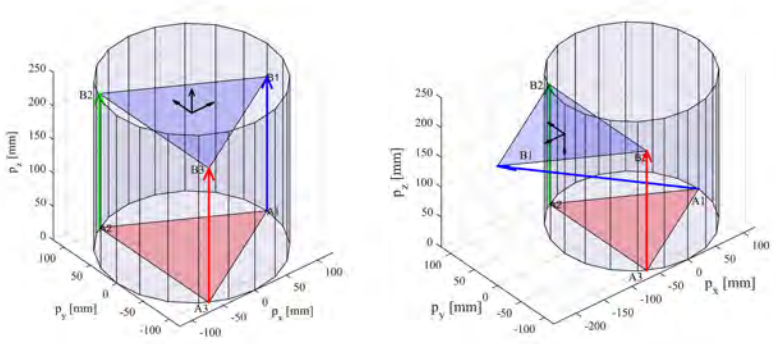

Figure 3: Theoretical workspace.

The computation of the working space through inverse kinematics and the fact that the limitations imposed by the joints are not taken into account are mentioned in Lukanin (2005). In the same work, it is shown that it is useful to discretize the leg lengths, solve for the direct kinematics and thus construct the boundary of the workspace as a set of discrete points in the cartesian space. This procedure avoids exploring solutions in the Cartesian space that are not feasible for the actual mechanism, thus reducing calculation efforts. In this work according to this approach, the mecanism workspace was constructed by discretization of the leg lengths in 1-mm steps, varying from 200 mm to 250 mm, totaling 50 points for each leg. Fig. 4 shows the practical workspace compared to the theoretical one, which is much larger.

Also from Fig. 4, it is clear that the centroid displacement is much smaller than those of the actuators' extremities, which emphasizes the utility of this mechanism for generating micro movements. The three-dimensional representation of the effective workspace is shown in Fig. 5.

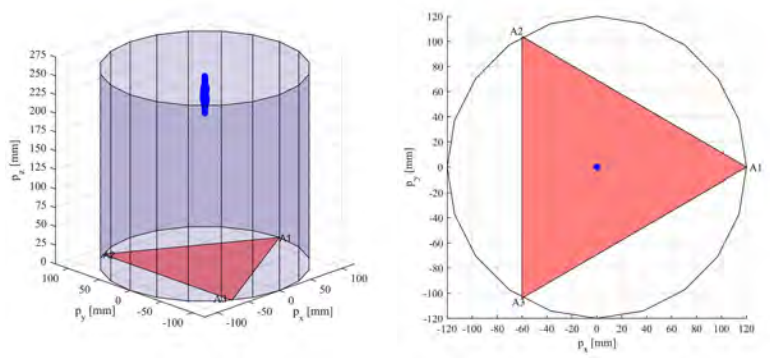

Figure 4: Effective workspace compared to the theoretical workspace.

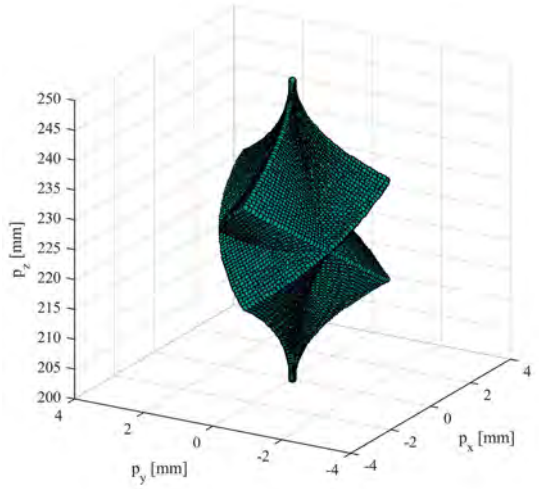

Figure 5: Effective workspace in detail.

The Fig. 6 shows in detail the workspace in the planes X-Y, X-Z and Y-Z. These views are helpful in further illustrating the micro movement characteristics of the mechanism. For instance, the values for p_x and p_y do not exceed 2,5 mm, for a 50-mm variation of the leg lengths. p_z is the only coordinate at the same scale of the variations of leg lengths.

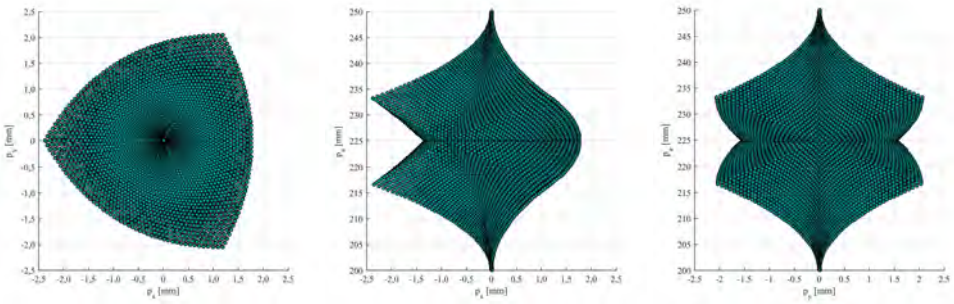

Figure 6: Effective workspace in planes X-Y, X-Z and Y-Z.

4. DYNAMICS

In this study, the dynamics of the mechanism is modeled according to the Lagrangian formulation, as described in detail in Almeida (2018). This methodology is widely used in the field of robotics, and in the specific case of the 3-RPS robot, similar methodologies can be found in Lee and Shah (1988) and Li and Xu (2005).

4.1 Lagrange's equations of the first kind

The main premise made in the discussion of the dynamics of the mechanisms is that all the elements are formed by rigid bodies. The Lagrange formulation is based on obtaining the kinetic and potential energies of each link of the manipulator. Once the energies are calculated the Lagrangian of the system is defined. The Lagrange equation is a function of the generalized coordinates $\mathbf{q}$ and their time derivative $\dot{\mathbf{q}}$, Eq.(9).

$$L(\mathbf{q}, \dot{\mathbf{q}}) = K - P \tag{9}$$

where K is the total kinematic energy and P the total potential energy of the system, $\mathbf{q}$ is the vector with the generalized coordinates and $\dot{\mathbf{q}}$ is its time derivative given in the Eq.(10).

$$\mathbf{q} = \begin{bmatrix} d_1 \\ d_2 \\ d_3 \\ \phi_1 \\ \phi_2 \\ \phi_3 \end{bmatrix} \quad , \quad \dot{\mathbf{q}} = \begin{bmatrix} \dot{d_1} \\ \dot{d_2} \\ \dot{d_3} \\ \dot{\phi_1} \\ \dot{\phi_2} \\ \dot{\phi_3} \end{bmatrix} \tag{10}$$

Eq.(9) is also known as the Second Type Lagrange Equation. However, as pointed out by Ghosal (2006), in parallel robots and closed-chain mechanisms, there are a number of chain closure constraint equations (also known as holonomic constraints) that are written as:

$$f_j(\mathbf{q}) = 0 \ , \quad j = 1, 2, 3 \tag{11}$$

The constraint equations, Eq.(11), are the same as the aforementioned Eq.(7). For the specific case of the 3-RPS mechanism the generalized coordinates are formed by three independent coordinates (d_1, d_2 and d_3) and three dependent coordinates (ϕ_1, ϕ_2 and ϕ_3). In this case, in order to obtain the equation of motion, the concept of Lagrange Multipliers is used. The following Eq.(12) is the Lagrange's equations of the first kind.

$$\overline{L}(\mathbf{q}, \dot{\mathbf{q}}) = L(\mathbf{q}, \dot{\mathbf{q}}) - \sum_{j=1}^{3} \lambda_j \frac{\partial f_j(\mathbf{q})}{\partial q_i} \ , \quad i, j = 1, 2, 3 \tag{12}$$

where λ_j are the Lagrange multipliers introduced and must be determined.

4.2 Obtaining kinematic and potential energy of the system

In order to obtain the differential equations a through the lagrange formulation it is necessary to obtain the kinetic and potential energies of the system. In this study, the parameters to calculate the dynamics of the manipulator considered masses and moments of inertia similar to the ones determined by Almeida (2018). The kinetic energy of the mobile platform is given by Eq.(13).

$$K_{plat} = \frac{1}{2} m \mathbf{V}^T \mathbf{V} + \frac{1}{2} \mathbf{\Omega}^T \mathbf{I} \, \mathbf{\Omega} \tag{13}$$

where, m is the mobile platform mass, $\mathbf{I}$ is the platform inertia tensor given by the Eq.(14), $\mathbf{V}$ and $\mathbf{\Omega}$ are the linear and angular velocities of the mobile platform respectively and are given by Eq.(15).

$$\mathbf{I} = {}^{A}_{B}\mathbf{R} \, \mathbf{I}_{local} \, {}^{A}_{B}\mathbf{R} \tag{14}$$

where $\mathbf{I}_{local}$ is the platform local inertia tensor.

$$\begin{bmatrix} V \\ \Omega \end{bmatrix} = \mathbf{J}(\mathbf{q}) \dot{\mathbf{q}} \tag{15}$$

where $\mathbf{J}(\mathbf{q})$ is the Jacobian matrix in generalized coordinates. The calculation of the Jacobian matrix can be found in Ghosal (2006) and Almeida (2018).

For the calculation of the kinetic energy of the legs, the premise to be made is that the distance to the rotational joint from the center of mass of each leg does not change with time. In this case the mass of the movable part of each actuator is neglected. This initial idea was proposed by Lee and Shah (1988), considering that most of the mass of the linear actuator

is in the lower part fixed to the rotational joint. The kinetic energy of the legs can then be described in matrix form in Eq.(16).

$$K_{leg} = \frac{1}{2} m_{leg} \mathbf{V}_{leg}^T \mathbf{V}_{leg} + \frac{1}{2} I_{leg} \dot{\phi}^T \dot{\phi} \tag{16}$$

where m_{leg} is the each leg mass, I_{leg} is the inertia momentum of each leg in relation to the revolute joint, $\mathbf{V_{leg}}$ is the vector containing the linear velocities of the center of mass of each leg given in Eq.(17) and $\dot{\phi}$ the vector containing the angular velocities of each leg given in Eq.(18).

$$\mathbf{V}_{leg} = r\dot{\phi} \tag{17}$$

where r is the distance from the center of mass of a leg relative to its respective rotational joint.

$$\dot{\phi} = \begin{bmatrix} \dot{\phi}_1 \\ \dot{\phi}_2 \\ \dot{\phi}_3 \end{bmatrix} \tag{18}$$

where $\dot{\phi}_i$ is the i^{th} leg angular velocity. The potential energy of the whole system is described through generalized coordinates. The potential energy of the mobile platform is given by Eq.(19)

$$P_{plat} = 9.81 \ \times \ p_z \tag{19}$$

The value of p_z can be calculated from the arithmetic mean of the spherical joint heights as show in Eq.(20)

$$p_z = \frac{1}{3}(d_1 sin(\phi_1) + d_2 sin(\phi_2) + d_3 sin(\phi_3)) \tag{20}$$

The potential energy of the leg set is given by Eq.(21).

$$P_{leg} = 9.81 \ \times \ r\, m_{leg}(sin(\phi_1) + sin(\phi_2) + sin(\phi_3)) \tag{21}$$

The kinetic energy and potential energy of the whole system are the sum of the kinetic and potential energy of the mobile platform and the leg set.

4.3 Inverse Dynamics

The problem of inverse dynamics consists in finding the values of torque and forces acting on a mechanism subjected to a trajectory as a function of time. The inverse dynamics in a robot, both serial and parallel, is solved directly since it involves the substitution $\mathbf{q}$, $\dot{\mathbf{q}}$ and $\ddot{\mathbf{q}}$ in the equation of motion and solve it for $\tau(t)$. The calculation of $\tau(t)$ is required for model-based control strategies such as Computed Torque. In addition, the maximum value of τ_t for a given trajectory required in design assists in the design and choice of actuators (Ghosal, 2006). Since the actuating forces components of the vector τ of legs 1, 2 and 3 are to be found for the 3-RPS mechanism, the leg lengths d_1, d_2 and d_3 are chosen as the independent generalized coordinates, and the angles formed by the leg and base ϕ_1, ϕ_2, and ϕ_3 are the dependent generalized coordinates. In this case the calculated forces will be those exerted by the prismatic joints. Since the kinetic energy depends on the generalized coordinates and their temporal derivatives, and while the potential energy depends only on the generalized coordinates, the motion equation can be as follows:

$$\frac{d}{dt}\left(\frac{\partial L}{\partial \dot{q}_i}\right) - \frac{\partial L}{\partial q_i} = \tau_i + \sum_{j=1}^{3} \lambda_j \frac{\partial f_j(\mathbf{q})}{\partial q_i} \ , \quad i = 1, 2, 3 \tag{22}$$

At this point it is possible to define some parameters presented in the Eq.(23).

$$\begin{aligned} q_i &= \begin{cases} d_i \ , & i = 1, 2, 3 \\ \phi_{i-3} \ , & i = 4, 5, 6 \end{cases} \\ \tau_i &= \begin{cases} F_i \ , & i = 1, 2, 3 \\ T_{i-3} \ , & i = 4, 5, 6 \end{cases} \end{aligned} \tag{23}$$

where, F_i is the acting force on the prismatic joint of the i^{th} leg and T_i is the friction torque of the i^{th} revolute joint. In this study, as in Lee and Shah, 1988b, due to the difficulty of modeling the friction losses, the frictional forces in the rotational

joints are considered zero. Solving Eq.(22), from the definitions of Eq.(23), it is possible to rewrite the equation as show in Eq.(24) and Eq.(25).

For $i = 1,\ 2,\ 3$

$$F_i = \frac{d}{dt}(\frac{\partial L}{\partial \dot{d}_i}) - \frac{\partial L}{\partial d_i} - (\lambda_1 \frac{\partial f_1(\mathbf{q})}{\partial d_i} + \lambda_2 \frac{\partial f_1(\mathbf{q})}{\partial d_i} + \lambda_3 \frac{\partial f_1(\mathbf{q})}{\partial d_i}) \tag{24}$$

For $i = 4,\ 5,\ 6$

$$\lambda_1 \frac{\partial f_1}{\partial \phi_{i-3}} + \lambda_2 \frac{\partial f_2}{\partial \phi_{i-3}} + \lambda_3 \frac{\partial f_3}{\partial \phi_{i-3}} = \frac{d}{dt}(\frac{\partial L}{\partial \dot{\phi}_{i-3}}) - \frac{\partial L}{\partial \phi_{i-3}} \tag{25}$$

The Eq.(25) is a set of three equations and three unknowns Lagrange multipliers λ_1, λ_2 and λ_3. Once obtained the Lagrange multipliers by the Eq.(25) it is possible to calculate the acting forces on the prismatic joints using Eq.(24).

In order to validate the mathematical model created a comparison with the results obtained by Sokolov, 2003, is made. In his work Sokolov (2013) got the dynamic model using virtual work approach. Sokolov (2013), also considers the mass of the mobile part of the actuators. This approach differs from the present work. To validate the model developed in this study, the same parameters of Sokolov (2013), ares used.

The forces acting on the prism joints are calculated from the imposition of a helical trajectory of the center of mass of the mobile platform. The helicoid pattern has radius r_h and pitch p_h and is given by the Eq.(26), Eq.(27) and Eq.(28).

$$p_x = r_h cos(\varphi) \tag{26}$$

$$p_y = r_h sin(\varphi) \tag{27}$$

$$p_z = z_0 + \frac{p_h}{2\pi}\varphi \tag{28}$$

where z_0 is the initial value of p_z and φ is given by Eq.(29).

$$\varphi(t) = \begin{cases} \frac{4\pi t^2}{\sqrt{1+9\pi^2}}, & 0 \geq t \geq t_a \\ \frac{\pi(4t-1)}{\sqrt{1+9\pi^2}}, & t_a \geq t \geq t_{a+b} \\ \frac{\pi(-2-9\pi^2+4(1+\sqrt{1+9\pi^2})t^2-4t^2)}{\sqrt{1+9\pi^2}}, & t_{a+b} \geq t \geq t_t \end{cases} \tag{29}$$

where t is time variable.

Fig. 7 shows the trajectory in the Cartesian space that must be developed by the centroid of the platform.

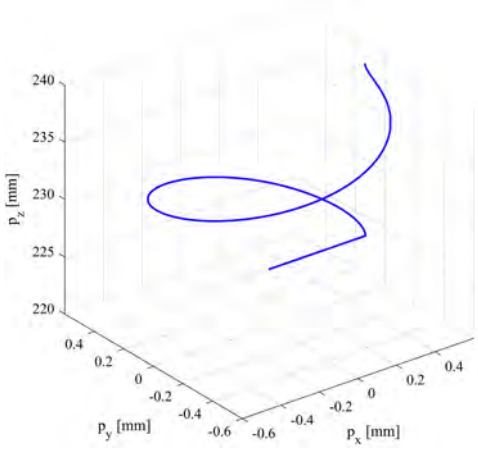

Figure 7: Helical trajectory in cartesian coordinates.

Tab. 1 shows the parameters taken from Sokolov (2013), and is used for the comparison of the methodologies. From the parameters for the simulation, Sokolov (2013), considers the masses and moments of inertia of the moving part of the linear actuators, not presented in the present study.

Fig. 8 shows the joint values (independent generalized coordinate path) for the helicoid trajectory. Although the methodolgy used by Sokolov (2013)is different from the one presented here, both kinematic approaches yield similar results.

Fig. 9 shows the force values in each linear actuator. The figure is complemented by the numerical values on Tab. 2. It is observed that the forces calculated here for each actuator resemble those given by Sokolov (2013), but are slightly smaller. An explanation for this is that in the study of Sokolov (2013), the mass and moments of inertia of the movable part of the actuators are considered, as previously exposed. In addition, the author makes use of virtual works for the calculation of the equation of movement.

Table 1: Parameters taken from Sokolov (2013), for validation of the mathematical model.

Manipulator parameters		
g	460	mm
h	230	mm
m	0.18	kg
$(I_{xx};\ I_{yy};\ I_{zz})$	$(0.093;\ 0.093;\ 0.187)$	$kg.m^2$
$(I_{xy};\ I_{xz};\ I_{yz})$	$(0;\ 0;\ 0)$	$kg.m^2$
r	200	mm
m_{leg}	0.09	kg
I_{leg}	0.05	$kg.m^2$
Manipulator parameters		
r_h	0.75	mm
p_h	0.5	mm
z_0	0.4	mm
Manipulator parameters		
t_a	0.5	s
t_b	4.2	s
t_t	5.2	s

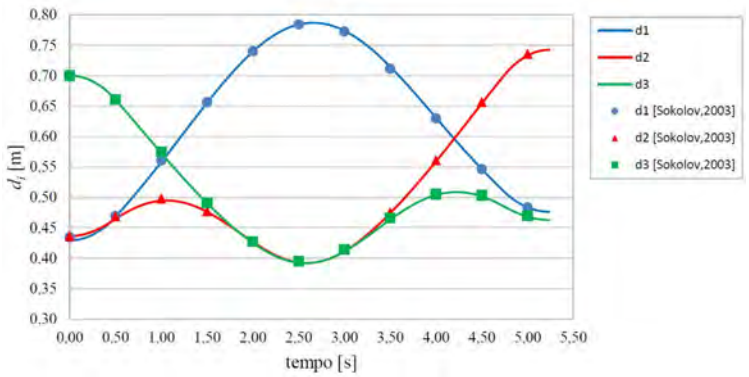

Figure 8: Inverse kinematics comparison.

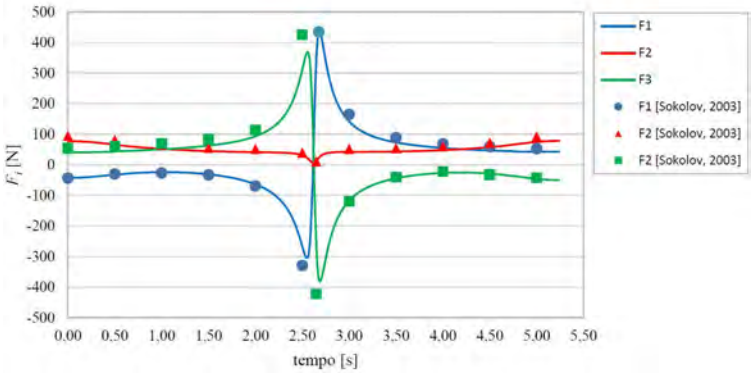

Figure 9: Inverse dynamics comparison.

Table 2: Comparison of minimum and maximum values of the acting force on the primitive joints.

	Sokolov, 2003			This study		
	d_1	d_2	d_3	d_1	d_3	d_3
Min	$-329\,N$	$11\,N$	$-422\,N$	$-305\,N$	$6\,N$	$-382\,N$
Max	$509\,N$	$95\,N$	$426\,N$	$438\,N$	$78\,N$	$369\,N$

5. CONCLUSIONS

In this study the kinematics calculation exposed the movement restrictions imposed by the configuration of the mechanism joints. It was possible to study the three independent degrees of freedom in the inverse kinematics and the difficulty

of solving the direct kinematics of the mechanism, where eight solutions were obtained for a given set of values of d_1, d_2 and d_3 being only one of them correct. The effective workspace of the mechanism was shown to be much more limited than its theoretical one. Thus, the main advantage of this mechanism lies in generating small displacements compared to those of its actuators. The dynamics of the mechanism was studied using the Lagrangian formulation. Its corresponding simulation results were compared to the bibliography, showing that the model represents satisfactorily the dynamic behavior of the mechanism.

6. REFERENCES

Almeida, M.V.G., 2018. *Estudo da Concepção de um Robô Paralelo de Três Graus de Liberdade*. Master's thesis, Universidade Federal do Rio Grande do Sul, Av. Paulo Gama, 110 - Farroupilha, Porto Alegre - RS.

Clavel, 1989. "Device for the movement and positioning of an element in space".

Dasgupta, B. and Mruthyunjaya, T., 2000. "The stewart platform manipulator: A review". *Mechanism and Machine Theory*, Vol. 35, pp. 15–40.

Ghosal, A., 2006. "A. robotics fundamental concepts and analysis". In *A. Robotics Fundamental Concepts and Analysis*. Oxford University Press.

Gosselin, C. and Hamel, J.F., 1994. "The agile eye: A high-performance three-degree-of-freedom camera-orienting device". In *The Agile Eye: A High-Performance Three-Degree-of-Freedom Camera-Orienting Device*. Vol. 1, pp. 781 – 786 vol.1.

H. Hunt, K., 1983. "Structural kinematics of in-parallel-actuated robot arms. trans asme j mech trans auto des". *Journal of Mechanisms Transmissions and Automation in Design*.

Huang, Z., Li, Q. and Ding, H., 2013. *Theory of parallel mechanisms*. Springer Verlag.

Lee, K.. and Shah, D.K., 1988. "Dynamic analysis of a three-degrees-of-freedom in-parallel actuated manipulator". *IEEE Journal on Robotics and Automation*, Vol. 4, No. 3, pp. 361–367. ISSN 0882-4967.

Li, Y. and Xu, Q., 2005. "Kinematics and inverse dynamics analysis for a general 3prs spatial parallel mechanism". *Robotica*, Vol. 23, pp. 219–229.

Lukanin, V., 2005. "Inverse kinematics, forward kinematics and working space determination of 3dof parallel manipulator with s-p-r joint structure". *Periodica Polytechnica Mechanical Engineering*, Vol. 49, No. 1, pp. 39–61. URL `https://pp.bme.hu/me/article/view/1341`.

Sokolov, A., 2013. *New Theoretical Approach for the Kinematics and Dynamics of 3-DOF Positioning Parallel Manipulators*. Ph.D. thesis, École Polytechnique Federale Lausanne.

Stewart, D., 1965. "A platform with six degrees of freedom". *Archive: Proceedings of The Institution of Mechanical Engineers 1847-1982 (vols 1-196)*, Vol. 180, pp. 371–386.

Tsai, L.W., 1999. "Robot analysis: The mechanics of serial and parallel manipulators". In *Robot Analysis: The Mechanics of Serial and Parallel Manipulators*. John Wiley Sons.

Wang, J. and Gosselin, C.M., 1997. "Kinematic analysis and singularity representation of spatial five-degree-of-freedom parallel mechanisms". *Journal of Robotic Systems*, Vol. 14, pp. 851–869.

Wang, J. and Gosselin, C.M., 1998. "A new approach for the dynamic analysis of parallel manipulators". *Multibody System Dynamics*, Vol. 2, pp. 317–334.

7. RESPONSIBILITY NOTICE

The authors are the only responsible for the printed material included in this paper.